Environmental and Molecular Mutagenesis 55:122–133 (2014)

Research Article

Effects of Silver Nanoparticles on Oxidative DNA Damage–repair as a Function of p38 MAPK Status: A Comparative Approach Using Human Jurkat T Cells and the Nematode *Caenorhabditis elegans*

Nivedita Chatterjee, Hyun Jeong Eom, and Jinhee Choi*

School of Environmental Engineering, Graduate School of Energy and Environmental system Engineering, University of Seoul, 163 Siripdaero, Dongdaemun-gu, Seoul 130–743, Korea

The large-scale use of silver nanoparticles (AgNPs) has raised concerns over potential impacts on the environment and human health. We previously reported that AgNP exposure causes an increase in reactive oxygen species, DNA damage, and induction of p38 MAPK and PMK-1 in Jurkat T cells and in *Caenorhabditis elegans*. To elucidate the underlying mechanisms of AgNP toxicity, here we evaluate the effects of AgNPs on oxidative DNA damage–repair (in human and *C. elegans* DNA glycosylases hOGG1, hNTH1, NTH-1, and 8-oxo-GTPases—hMTH1, NDX-4) and explore the role of p38 MAPK and PMK-1 in this process. Our comparative approach examined viability, gene expression, and enzyme activities in wild type (WT) and p38 MAPK knock-down (KD) Jurkat T cells (in vitro) and in WT and *pmk-1* loss-of-function mutant strains of *C. elegans* (in vivo). The results suggest that p38 MAPK/PMK-1 plays protective role against AgNP-mediated toxicity, reduced viability and greater accumulation of 8OHdG was observed in AgNP-treated KD cells, and in *pmk-1* mutant worms compared with their WT counterparts, respectively. Furthermore, dose-dependent alterations in hOGG1, hMTH1, and NDX-4 expression and enzyme activity, and survival in *ndx-4* mutant worms occurred following AgNP exposure. Interestingly, the absence or depletion of p38 MAPK/PMK-1 caused impaired and additive effects in AgNP-induced *ndx-4*(*ok1003*); *pmk-1*(RNAi) mutant survival, and hOGG1 and NDX-4 expression and enzyme activity, which may lead to higher accumulation of 8OHdG. Together, the results indicate that p38 MAPK/PMK-1 plays an important protective role in AgNP-induced oxidative DNA damage–repair which is conserved from *C. elegans* to humans. Environ. Mol. Mutagen. 55:122–133, 2014.

Key words: 8OHdG; DNA glycosylases; 8-oxo-GTPases; silver nanoparticles; p38 MAPK; PMK-1

INTRODUCTION

The antimicrobial properties of silver nanoparticles (AgNPs) (Feng et al., 2000; Kim et al., 2007) have been exploited in various industries including textile, food, paints, cosmetics, electronics, coatings, water purification, and biomedical products (Chen and Schluesener, 2008; Ahamed et al., 2010a). With increased commercialization there is a corresponding increase in human exposure, and as such, health and environmental risk assessments are necessary (Ahamed et al., 2010a). In this regard, it has been documented that the possible mechanisms of AgNP toxicity include the induction of reactive oxygen species

Additional Supporting Information may be found in the online version of this article.

Abbreviation: AgNPs, silver nanoparticles; *C. elegans*, *Caenorhabditis elegans*; hMTH1, 8-oxo-GTPase, MutT homolog 1 or NUDT1; hNTH1, human NTHL1 nth endonuclease III-like 1; hOGG1, human 8-oxoguanine DNA glycosylase 1; NDX-4, *C. elegans* 8-oxo-GTPase, MutT homolog 1; NTH-1, *C.elegans* NTHL1 nth endonuclease III-like 1; 8OHdG, 8-Hydroxydeoxyguanosine; ROS, reactive oxygen species.

Conflict of interest statement: The authors declare no conflict of interest.

Grant sponsor: Mid-career Researcher Program through the National Research Foundation of Korea (NRF) funded by the Ministry of Science, ICT, and Future Planning; Grant number: 2013R1A2A2A03010980.

Grant sponsor: the Korea Ministry of Environment as "Environmental Health R&D Program"; Grant number: 2012001370009.

*Correspondence to: J. Choi. E-mail: jinhchoi@uos.ac.kr

Received 16 September 2013; provisionally accepted 19 November 2013; and in final form 1 December 2013

DOI 10.1002/em.21844

Published online 18 December 2013 in Wiley Online Library (wileyonlinelibrary.com).

(ROS), oxidative stress, DNA damage, and apoptosis in a wide range of model systems, including cultured mammalian cells, *C. elegans*, mouse, zebrafish, rainbow trout, fruitfly, microbes, etc. (Hwang et al., 2008; AshaRani et al., 2009; Rahman et al., 2009; Roh et al., 2009; Ahamed et al., 2010b; Choi et al., 2010; Scown et al., 2010; Kim et al., 2011; Yang et al., 2012). In addition, activation of stress-responsive mitogen-activated protein kinases (MAPKs), such as JNK and p38 MAPK, has been reported as a possible consequence of the oxidative stress-induced by AgNPs (Hsin et al., 2008; Piao et al., 2011a; Kang et al., 2012). In this context, we previously reported the specific activation and phosphorylation of p38 MAPK among all of the stress-mediated MAPKs (i.e., JNK and ERK-1/2), ROS generation and induction of DNA damage in AgNP-treated Jurkat T cells (Eom and Choi, 2010). This is further supported by our recent study on the effects of AgNPs in *C. elegans*, which demonstrated oxidative stress and activation of PMK-1, the *C. elegans* ortholog of p38 MAPK (Lim et al., 2012).

The p38 MAPKs are a class of evolutionarily conserved serine/threonine MAPKs that are involved in the coordination of extracellular signals and intracellular machinery required to regulate a plethora of cellular processes. The mammalian p38 family (α, β, γ, δ) has been linked to the activation of inflammation, cell cycle, cell death, development, cell differentiation, senescence, and tumorigenesis in specific cell types (Zarubin and Han, 2005; Coulthard et al., 2009; Cuadrado and Nebreda, 2010). Comparably, PMK-1 has been identified as a key protein involved in pathogen defense and innate immunity in worms (Kim et al., 2002; Troemel et al., 2005). Interestingly, p38 MAPK/PMK-1 can be phosphorylated and activated by a wide range of external stimuli, including oxidative stress (Martindale and Holbrook, 2002; Inoue et al., 2005; Kondo et al., 2005; McCubrey et al., 2006). Based on the accumulated ROS burden, oxidative stress may either activate MAPK pathways toward proliferation and survival, or initiate cell death by causing severe damage to cellular macromolecules such as DNA, protein, and lipids (Martindale and Holbrook, 2002).

Oxidative DNA damage, which includes oxidized DNA bases, apurinic/apyrimidinic (AP) sites and DNA single-strand breaks, is an inevitable consequence of endogenous metabolism. Oxidative DNA damage increases following exogenous toxic insult and is implicated in the etiology of many diseases (including cancer, neurodegenerative disorders, and cardiovascular disease) and in aging. The removal of oxidized bases is performed predominantly by the base excision repair (BER) pathway, which is evolutionarily conserved from *Escherichia coli* to humans (Cooke et al., 2003; Izumi et al., 2003; Powell et al., 2005; Hazra et al., 2007). Several related but distinct DNA glycosylases initiate the BER process by releasing modified bases. Two mammalian glycosylases, 8-oxoguanine DNA glycosylase (OGG1) and nth endonuclease III-like 1, *E. coli* (NTH1), are documented to excise the majority of the oxidatively damaged base lesions (Wood et al., 2001; Cooke et al., 2003; Hazra et al., 2007). Furthermore, another mammalian enzyme, MutT homolog 1 (MTH1), is responsible for 8-oxoGTPase activity and removal of 8-OH-dGTP from nucleotide pools (Wood et al., 2001; Cooke et al., 2003). Similarly, the *C. elegans* homolog of NTH1 (*nth-1*) is a highly conserved DNA glycosylase that removes oxidatively damaged pyrimidine bases (Morinaga et al. 2009), and the *C. elegans ndx-4* gene exhibits the hallmarks of a MutT-type enzyme with an ability to hydrolyze 8-OH-dGTP (Arczewska et al., 2011).

Modulations of BER enzymes have been reported as an important risk factor for human cancer (Tudek, 2007). Therefore, toxicants that cause alterations in BER enzymes require great attention. Moreover, it is important to elucidate the interaction of BER enzymes with, and regulation by, other proteins. An association between MAPK (p38 MAPK and ERK1/2) and hOGG1 proteins has been reported to counteract hyperoxic toxicity in A549 cells and primary AECII cells (Kannan et al., 2006). Conversely, to the best of our knowledge, no direct interaction either between p38 MAPK and hMTH1, or between PMK-1 and NTH-1/NDX-4, has been documented. In particular, Cuadrado and Nebreda (2010) raised a very interesting point in their recent review detailing how p38 MAPK may modulate a number of proteins without phosphorylating them, and discuss the large number of p38 MAPK's substrates for phosphorylation that range from protein kinases to transcription factors (Cuadrado and Nebreda, 2010).

We hypothesized that p38 MAPK and PMK-1 are involved in AgNP-induced toxic responses that are conserved from *C. elegans* to humans. The objective of the present study was to evaluate whether and how p38 MAPK/PMK-1 is involved in AgNP-induced oxidative DNA damage–repair and, in addition, the nature of its conservation from the nematode *C. elegans* to humans. Our approach was comparative and we used wild type (WT) and p38 MAPK knock-down (KD) Jurkat T cells (siRNA transfection) as an in vitro model system, and WT (*N2*) and *pmk-1* (*km25*) mutant strains (details in Supporting Information Table-S1) of *C. elegans* as an in vivo model system.

MATERIALS AND METHODS

Cell Culture and p38 MAPK siRNA Transfection

Jurkat T (human lymphoma) cells were grown in RPMI 1640 (GIBCO, Carlsbad, CA) supplemented with 10% heat-inactivated fetal bovine serum, 1% penicillin–streptomycin, at 37°C in a humidified atmosphere containing 5% CO_2. To achieve the desired p38 MAPK gene silencing, cells were transfected (reverse transfection) with predesigned double-stranded siRNAs that selectively target total MAPK14 gene (p38 MAPK) (product ID s3586, Ambion, Austin, TX). The transfection method was optimized by following the instruction provided by transfection reagent

supplier (Mirus Bio LLC, Madison, WI). Briefly, 10 μL of TransIT-TKO transfection reagent (MIR-2150, Mirus Bio LLC) was added to 250 μL of serum-free medium (room temperature), mixed with ds-siRNA (100 nM) and added to a six-well plate after 30 min of incubation. Approximately, 3×10^6 cells in 1.25 mL RPMI 1640 (antibiotic free) were added dropwise into the well containing siRNA. The efficiency of siRNA-mediated translational silencing was monitored by immunoblot analysis and maximal suppression was observed at 48 hr (Supporting Information Fig. S1). After 48 hr, transfected cells were used for AgNP treatment.

AgNPs Preparation and Cell Treatment

AgNPs were prepared as described previously (Eom and Choi, 2010) (a precise description is available in Supporting Information, Section 1.1). If not otherwise stated, both kind of cells, WT and p38 MAPK siRNA KD, were treated with two AgNP concentrations, 0.05 mg/L (EC_{10}) and 0.25 mg/L (EC_{50}) for 24 hr. The EC_{10} and EC_{50} were used from our previous study (Eom and Choi, 2010).

Cell Viability

WT and KD Jurkat T cells were plated on six-well plates at 1×10^6 cells/mL and were treated with 0.05 and 0.25 mg/L AgNPs for 24 hr. Treated and control cells were stained with 0.4% trypan blue (Invitrogen, Carlsbad, CA) and the total number of stained and unstained cells was counted using a hemocytometer. All experiments were performed in triplicates.

Caenorhabditis elegans Maintenance and Treatment with AgNPs

Caenorhabditis elegans were grown in petri dishes on nematode growth medium and fed with the OP50 strain of *E. coli* according to a standard protocol (Brenner, 1974). Worms were incubated at 20°C, with young adults (3-day-old) from an age-synchronized culture then used in all the experiments. WT (*N2*), *pmk-1* (*km25*), *ndx-4* (*ok1003*), and *nth-1* (*ok724*) mutants were provided by the Caenorhabditis Genetics Center (www.CGC.org, Supporting Information Table S1) at the University of Minnesota. For *C. elegans treatment*, AgNPs were prepared and characterized as described previously (Eom et al., 2013) (a brief description is available in Supporting Information, Materials and Methods, Section 1.2). Worms were treated for 24 hr with two AgNP concentrations, 0.025 mg/L (LC_{10}) and 0.05 mg/L (LC_{50}), mixed in EPA water ($NaHCO_3$ 96 mg/L, $CaSO_4 \cdot 2H_2O$ 60 mg/L, $MgSO_4$ 60 mg/L, and KCl_4 mg/L).

PMK-1 RNA Interference (RNAi)

The PMK-1 RNAi feeding was performed on *ndx-4* (*ok1003*) and *nth-1* (*ok724*) mutant *C. elegans*, as previously described (Lim et al., 2012). The RNAi bacteria were induced for 48 hr at room temperature for dsRNA expression. The L3/L4-stage worms were then added onto the RNAi plate and incubated at 20°C. After 36–40 hr of incubation, worms were transferred to another large-scale plate seeded with the same RNAi bacteria and then the worms were grown to adult. The adult worms were then age-synchronized and the eggs were seeded to new, freshly prepared, *pmk-1* RNAi feeding plates. The efficiency of RNAi interference was assessed by quantitative real-time PCR (qRT-PCR) with corresponding *pmk-1* gene primers (Supporting Information Fig. S2).

Survival Assay

The WT (*N2*), *pmk-1*, *ndx-4* (*ok1003*), and *nth-1* (*ok724*) mutants, as well as *ndx-4*; *pmk-1* RNAi and *nth-1*; *pmk-1* RNAi worms, were assessed after 24 hr exposures to 0.025 mg/L (LC_{10}) and 0.05 mg/L (LC_{50}) AgNPs mixed in EPA water. Survival was assessed by counting the number of live and dead individuals under a dissecting microscope, while probing the worms with a platinum wire (Roh et al., 2009). LC_{10} and LC_{50} were measured from *N2 C. elegans* exposed to a range of AgNP concentrations (data not shown).

8-Hydroxydeoxyguanosine (8-OHdG) Measurement

8-OHdG detection was carried out using Oxiselect™ Oxidative DNA damage ELISA Kits (Cell Biolabs, Inc., San Diego, CA). The process was conducted in three major steps: DNA extraction, DNA digestion, and 8-OHdG detection. Detailed methodologies are in the Supporting Information.

Quantitative Real-time PCR (qRT-PCR)

Total RNA from all samples (WT and KD Jurkat T cells, *N2* and *pmk-1* mutant *C. elegans*) was extracted using RNA extraction kits (NucleoSpin, Macherey-Nagel, Düren, Germany). The quantity and quality of RNA was detected using a spectrophotometer and by agarose gel separation.

Synthesis of cDNA was performed by a reverse transcriptase (RT) reaction and PCR amplification was carried out with a thermal cycler (Bio-Rad, Hercules, CA). The qRT-PCR analysis was accomplished with CFX manager (Bio-Rad, Hercules, CA) using the IQ™ SYBR Green SuperMix (Bio-Rad, Hercules, CA). The primers were constructed (by Primer3plus) based on sequences available in NCBI and the qRT-PCR conditions were optimized (efficiency and sensitivity tests) for each primer prior to the experiment (Supporting Information Tables S2 and S3). Three biological replicates each were run in triplicates for each qRT-PCR analysis. Analysis of negative control reactions (minus RT and all reagents minus template) confirmed no DNA contamination. Gene expression was normalized using GAPDH (for human cells) and *gpd-1* (for *C. elegans*) as housekeeping genes.

Human 8oxo-G DNA Glycosylase-1 (hOGG1) Activity Assay

The 8oxo-G DNA glycosylase-1 (hOGG1) activity assays were measured colorimetrically as described by Liu et al. (2013) with some modification. Briefly, AgNP-exposed cell pellets (WT and KD cells) were combined with equal volumes of extraction buffer (50 mM Tris-HCl pH 7.5, 150 mM NaCl, 0.05% NP-40, 2 mM EDTA, phenylmethylsulfonyl fluoride [PMSF]) and crude cell lysates prepared by incubating 30 min in ice with frequent vortexing followed by centrifuged at 20,000*g*, 30 min, 4°C. Protein concentrations were determined using the Bradford Reagent (BioRad, Hercules, CA). Thereafter, 5 μL DNA-1 (modified with *8oxoG*) (10 μM), 5 μL DNA-2 (10 μM), 5 μL NEBuffer2 (10×), and 32.5 μL H_2O were incubated at 90°C for 5 min then slowly cooled to room temperature. BSA (10 μg/mL final), five units of λ exonuclease (New England BioLabs Inc., Ipswich, MA) and 20 μg of protein (optimized with varying concentrations of proteins ranging from 1 to 100 μg, data not shown) were added to give a reaction volume of 50 μL and the reaction mixture was incubated at 37°C for 40 min. After that 15 μL of 5 μM hemin, 75 μL of 2× HEPES (25 mM HEPES, 200 mM NaCl, 10 mM KCl, 0.05% triton, pH 5.2) solution and 10 μL H_2O were added and incubated at room temperature for 30 min. Absorption spectra were recorded at 410 nm within 600 sec after the addition of 20 μL of 20 mM ABTS and 20 μL of 10 mM H_2O_2. The background and the details of the experiment can be found in Supporting Information.

8-oxo-dGTPases (Human MutT Homolog [hMTH1] and C. elegans MutT Homolog [NDX-4]) Activity Assay

8-oxo-dGTPases hMTH1 and NDX-4, activity assays were carried out as described by Bialkowski and Kasprzak (1998) and Arczewska

et al. (2011), respectively, with some modifications. Briefly, the AgNP-exposed homogenized worm pellets (*N2* and *pmk-1* mutant) or cell pellets (WT and KD cells) were combined with equal volumes of extraction buffer (50 mM Tris-HCl pH 7.5, 150 mM NaCl, 0.05% NP-40, 2 mM EDTA, PMSF) and crude lysates prepared by incubating 30 min in ice with frequent vortexing followed by centrifuged at 20,000*g*, 30 min, 4°C. Protein concentrations were determined using the Bradford Reagent (BioRad, Hercules, CA). Twenty micrograms of protein (optimized with varying concentrations of proteins ranging from 1 to 100 μg, data not shown) was mixed with 250 μM 8-oxodGTP (TriLink Biotechnologies, San Diego, CA) in reaction buffer (5 mM $MgCl_2$, 40 mM NaCl, 50 mM Tris-HCl, pH 8) in a total volume of 50 μL and incubated for 2 hr at 37°C. Thereafter, 0.1 U/μL of inorganic pyrophosphatase (New England BioLabs Inc., Ipswich, MA) was added to the reaction mixture and incubated for another 20 min at 37°C to convert pyrophosphates to free phosphates. At the end of the incubation period, free phosphates were quantified colorimetrically using the Biomol Green™ (Enzo Life Sciences International, Farmingdale, NY) phosphate detection method. One-hundred microliters of the Biomol Green reagent was added to the each reaction mixture (50 μL) and the mixture was incubated for 20 min at room temperature. The change in absorbance at 620 nm was measured and used to determine free phosphate concentrations by comparison with a standard curve. Free phosphate from sources other than 8-oxo-dGTPases was corrected with a reaction well containing all reagent excluding the substrate, 8-oxodGTP.

Antioxidant N-acetyl Cysteine (NAC) Treatment

To investigate the role of oxidative stress in AgNP-induced toxicity, WT and KD Jurkat T cells and *C. elegans* were pretreated with 10 mg/L NAC for 2 hr followed by simultaneous treatment with higher concentrations (0.25 mg/L in cells and 0.05 mg/L in worms) of AgNPs. After 24 hr exposure, the cells and the worms were checked for viability/survival, oxidative DNA damage–repair, and enzyme activity.

Statistical Analysis

The statistical significance of differences among/between treatments was determined using one way analysis of variance (ANOVA). This was followed by a post-hoc test (Tukey, $P < 0.05$). All statistical analyses were carried out using SPSS 12.0KO (SPSS Inc.) and graphs were prepared in SigmaPlot (Version 12.0).

RESULTS AND DISCUSSION

AgNP Characterization

For Jurkat T cells exposure, the shape and size distribution of AgNPs in cell culture medium (RPMI 1640) was determined under cell-free conditions. Dynamic light scattering (DLS) indicated that the sizes of the main NPs distributed in the medium were approximately 28–35 nm, having a zeta potential value of −30 mV (Supporting Information, Figs. S3A and S3B; for details please refer to Eom and Choi [2010]). For *C. elegans* treatment, AgNPs dispersed in EPA water and measured by DLS were found to have a hydrodynamic diameter of approximately 100–150 nm (122.30 ± 4.16) (Supporting Information Fig. S3D). The zeta potential of the AgNPs in EPA water was found to be around −25 mV (−24.13 ± 0.62). In addition, the TEM images of the AgNPs showed a diameter of 20 nm and the secondary AgNPs were loosely aggregated (Supporting Information Fig. S3C; for details please refer to Eom et al. [2013]).

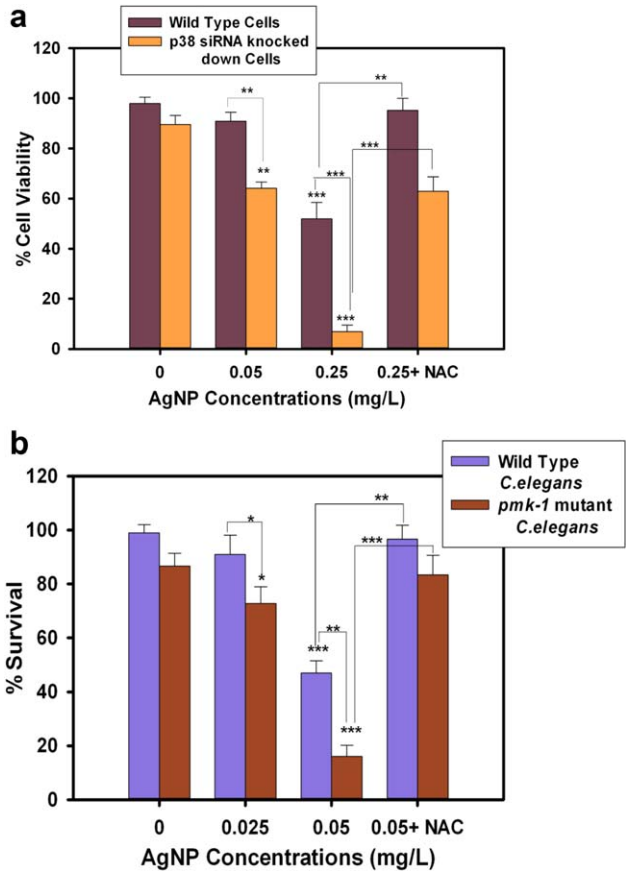

Fig. 1. a. Cell viability (%) of WT and p38 MAPK siRNA KD Jurkat T cells following 24 hr AgNP exposures at two different concentrations (0.05 and 0.25 mg/L) measured by trypan blue exclusion. NAC pretreatment rescued viability. Data presented as mean ± SEM. $*P < 0.05$, $**P < 0.001$, $***P < 0.0001$. b. Survival (%) of WT (*N2*) and *pmk-1* mutant (*km25*) *C. elegans* due to 24 hr AgNPs exposures at two different concentrations (0.025 and 0.05 mg/L) by counting the viable and the dead worms under microscope. NAC pretreatment rescued survival. Data presented as mean ± SEM. $*P < 0.05$, $**P < 0.001$, $***P < 0.0001$. [Color figure can be viewed in the online issue, which is available at wileyonlinelibrary.com.]

Role of p38 MAPK/PMK-1 in AgNP-mediated Toxicity in Jurkat T Cells and *C. elegans*

In order to evaluate the role of p38 MAPK, we compared the effects of AgNP-induced cell viability in WT and KD Jurkat T cells at two different concentrations: 0.05 mg/L (EC_{10}) and 0.25 mg/L (EC_{50}) (concentrations established in our previous study [Eom and Choi, 2010]). Interestingly, KD cells exhibited much greater sensitivity than WT cells at the same concentration of AgNPs. Specifically, upon treatment at the EC_{50} of the WT cells, almost all of the KD cells were dead (Fig. 1a). Since

there were no marked differences in observed viability between WT and KD controls, p38 MAPK presumably protects cells only from environmental insults (i.e., AgNPs) but not from damage induced by endogenous factors. In the same way, a protective role of p38 against AgNP-mediated toxicity in SK-OV3 cells by activation of Nrf-2/HO-1 pathway has previously been shown (Kang et al., 2012). To compare in vivo–in vitro responses of p38 MAPK in AgNP-induced toxicity, we used *N2* and *pmk-1* mutant (*km25) C. elegans* strains exposed to two different concentrations of AgNPs: 0.025 mg/L (LC_{10}) and 0.05 mg/L (LC_{50}) dissolved in EPA water (unpublished data). In keeping with results in the Jurkat T KD cells, *pmk-1* mutant strains displayed a dose-dependent increase in susceptibility (Fig. 1b). Hence, we postulated that PMK-1 not only protects worms from pathogens (Troemel et al., 2005), but also from other external stimuli such as AgNPs. Furthermore, antioxidant NAC treatment prior to exposure to the higher concentration of AgNPs rescued AgNP-induced toxicity in both cell types (Fig. 1a) and in both nematode strains (Fig. 1b).

The above results are in agreement with Yang et al. (2012), who reported that NAC not only rescued mortality but also restored nematode growth. Piao et al. (2011a) hypothesized that the suppression of reduced glutathione (GSH) was one of the main mechanisms of AgNP toxicity in human Chang liver cells. The rescue of viability/survival following NAC pretreatment was much more significant in AgNP-exposed KD cells and *pmk-1* mutant strains (Figs. 1a and 1b) than in AgNP-exposed WT counterparts (Figs. 1a and 1b). These findings suggest a pro-survival role of p38MAPK/PMK-1, particularly under oxidative stress conditions. The p38 MAPK gene is known to confer resistance to oxidative stress (Cai et al., 2011) and increases cell survival [p38 (α)] in response to oxidative stress via the induction of antioxidant genes (Gutierrez-Uzquiza et al., 2012). In a similar manner, the PMK-1 pathway regulates oxidative stress response via the transcription factor *skn-1* in *C. elegans* (Inoue et al., 2005). In short, p38 MAPK and the *C. elegans* ortholog PMK-1 shared conserved protective roles in AgNP-mediated oxidative stress.

We hypothesized that oxidative DNA damage is one of the main reasons behind the reduced viability/survival of the model systems, and accordingly, we sought to investigate oxidative DNA damage and repair.

p38 MAPK / PMK-1 Dependent Changes in AgNP-induced Oxidative DNA Damage and Repair

8-OHdG Formation

The levels of 8-OHdG, an established marker of oxidative stress-induced DNA base lesions (Cadet, 2003; Valavanidis et al., 2009), were determined in both Jurkat T cells and in *C. elegans*. AgNP exposure caused a concentration-dependent increase in the levels of 8-OHdG adducts in Jurkat T cells (WT and KD), and the degree of 8-OHdG accumulation was much higher in KD cells (Fig. 2a). In a similar way, both strains of *C. elegans* (*N2* and *pmk-1* mutant) displayed a dose-dependent increase in 8-OHdG formation, with a higher frequency occurring in *pmk-1* mutant worms (Fig. 2b). DNA double strand breaks and p53 protein upregulation has been reported in AgNP-treated mouse embryonic stem cells (Ahamed et al., 2008) and specifically, increased levels of 8-oxoG in AgNP-exposed human Chang liver cells (Piao et al., 2011b). Moreover, our recent study has shown that AgNP

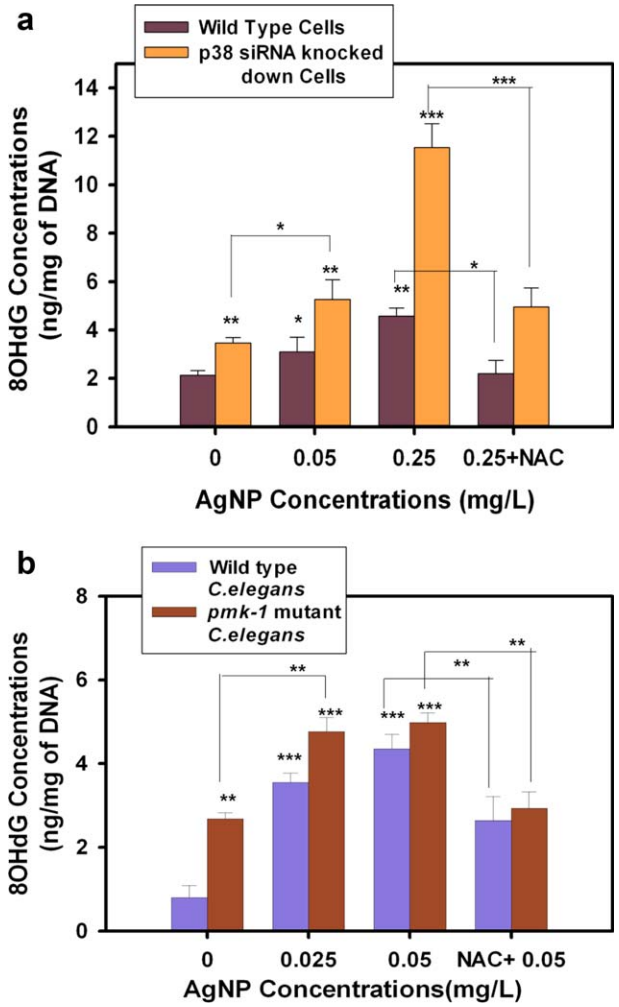

Fig. 2. a. 8-hydroxyguanosine (8-OHdG) (ng/mg of DNA) in WT and p38 MAPK siRNA KD Jurkat T cells treated with two different concentrations (0.05 and 0.25 mg/L) of AgNPs for 24 hr. 8-OHdG was measured using Oxiselect™ Oxidative DNA damage ELISA kits. NAC pretreatment decreased 8OHdG levels. Data presented as mean ± SEM. $*P < 0.05$, $**P < 0.001$, $***P < 0.0001$. b. 8-hydroxyguanosine (8-OHdG) (ng/mg of DNA) in WT (*N2*) and *pmk-1* mutant *(km25) C. elegans* following treatment with AgNPs for 24 hr at different concentrations measured using Oxiselect™ Oxidative DNA damage ELISA kits. NAC pretreatment decreased 8-OHdG levels. Data presented as mean ± SEM. $*P < 0.05$, $**P < 0.001$, $***P < 0.0001$. [Color figure can be viewed in the online issue, which is available at wileyonlinelibrary.com.]

exposure induces oxidative DNA damage as measured by 8-hydroxyguanosine (8-OHdG) concentrations in WT (*N2*) *C. elegans* (unpublished data).

Antioxidant NAC pre-treatment revealed a remarkable reduction in the levels of 8-OHdG in both cell types as well as in worms (Figs. 2a and 2b). These findings corroborate that ROS generation is involved in AgNP-mediated DNA damage, as was observed by Kang et al. (2012) in AgNP-treated SK-OV3 cells.

Two main mechanism are known to be involved in 8-OHdG formation and excision: (1) the direct oxidation of guanine bases in DNA that are excised and repaired by the initiator of the BER pathway, the 8oxo-G DNA glycosylase 1 (OGG1); and (2) the misincorporation of an oxidized dGTP (8-oxo-dGTP) during DNA synthesis, which is known to be prevented by the 8-oxo-GTPase MutT homolog (MTH1) (Cooke et al., 2003; Paz-Elizur et al., 2008; Svilar et al., 2011).

It has been proposed that the expression of base excision DNA repair genes may provide sensitive biomarkers for the detection of chemically induced oxidative DNA damage (Rusyn, 2004; Powell et al., 2005). Thus, we sought to quantify changes in the expression and activity of the genes involved in 8-OHdG excision and repair in both Jurkat T cells and the orthologs of those genes in the nematode *C. elegans*, as a cause of significant accumulation of AgNP-induced 8-OHdG.

Human 8oxo-G DNA Glycosylase-1 (hOGG1)

AgNP exposure caused a highly significant ($P < 0.001$) dose-dependent decrease in hOGG1 gene expression (~2.3 fold in WT and ~5 fold in KD cells at 0.25 mg/L) in Jurkat T cells (WT and KD) (Fig. 3a). Conversely, NAC treatment rescued hOGG1 expression in controls (without AgNP treatment). This decreased gene expression phenomenon was further supported by hOGG1 repair activity (Fig. 3b) induced following AgNP exposure in both types of Jurkat T cells (WT and KD). The AgNP treatment caused a significant increase in repair activity at the lower concentration (0.05 mg/L), followed by a sharp decrease at the higher concentration (0.25 mg/L) in WT cells. Therefore, we postulated that the decreased gene expression and subsequent attenuated activity of hOGG1 in AgNP-treated cells led to increased 8-OHdG levels. A decrease in hOGG1 gene expression and cleavage activity due to the arsenic exposure in A549 cells has been documented (Ebert et al., 2011). Our results are in agreement with the findings of Piao et al. (2011b), who reported that exposure to AgNPs caused downregulation of hOGG1 expression in human Chang liver cells by decreasing Nrf2 binding to the hOGG1 gene promoter. Most importantly, our data revealed a remarkable difference in hOGG1 gene expression and repair activity between KD cells and WT Jurkat T cells both in controls as well as in AgNP-exposed cells; these differences became more profound

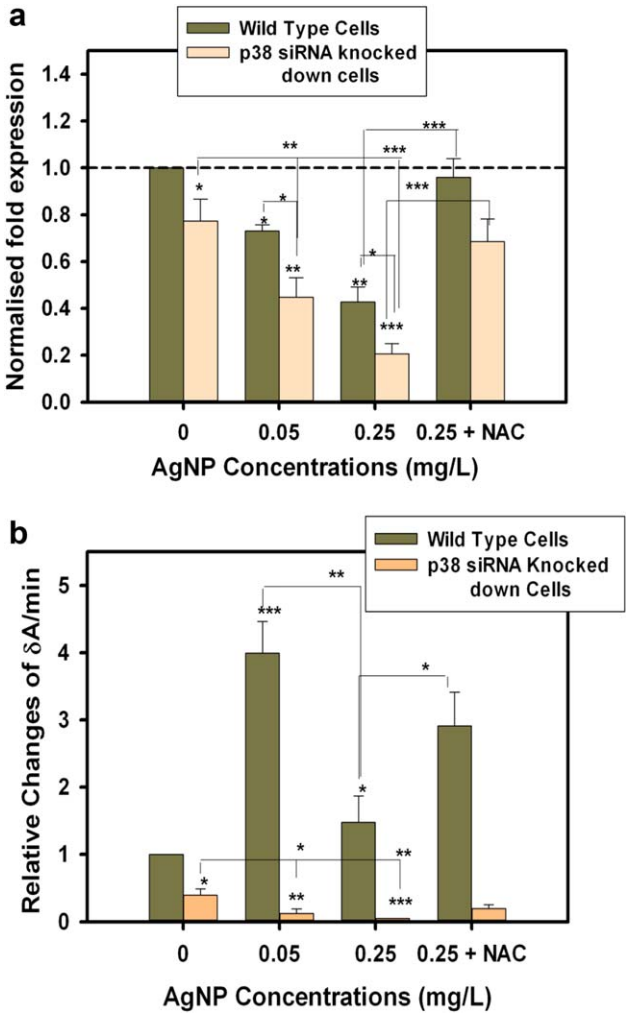

Fig. 3. a. hOGG1 gene expression in WT and p38 MAPK KD Jurkat T cells following 24 hr AgNP exposure at two different concentrations (0.05 and 0.25 mg/L) measured by qRT-PCR. NAC pretreatment rescued hOGG1 gene expression. Data presented as mean ± SEM. $*P < 0.05$, $**P < 0.001$, $***P < 0.0001$. b. Measurement of hOGG1 repair activity in WT and p38 MAPK KD Jurkat T cells following 24 hr AgNP exposure at two different concentrations (0.05 and 0.25 mg/L) using colorimetrically based on HRP-mimicking DNAzyme coupled with lambda exonuclease (λ exo) cleavage as described by Liu et al. (2013). NAC pretreatment rescued the hOGG1 activity. Data presented as mean ± SEM. $*P < 0.05$ $**P < 0.001$, $***P < 0.0001$. [Color figure can be viewed in the online issue, which is available at wileyonlinelibrary.com.]

with increasing concentrations of AgNPs (Figs. 3a and 3b) and p38 MAPK knock-down caused an additive effect in AgNP-induced hOGG1 down-regulation, and consequently, increased 8OHdG formation in KD cells (Fig. 2a). Therefore, there might be a connection between hOGG1 and p38 MAPK, as reported by Kannan et al. (2006).

Since the hOGG1 ortholog in *C. elegans* is unknown (Morinaga et al., 2009; Arczewska et al., 2011), we evaluated 8-oxo-dGTPase expression in both systems as a possible cause for 8-OHdG accumulation.

hMTH1, the 8-oxo-dGTPases

Given that AgNPs impaired hOGG1 expression and its p38 dependency, we felt it necessary to establish the interaction between AgNPs and hMTH1 expression, which possesses broader substrate specificity than its *E. coli* counterpart and dephosphorylates 8-oxodATP and 2-oxodATP with comparable efficiency to its cognate substrate 8-oxodGTP (Fujikawa et al., 1999). hMTH1 expression is an established molecular marker of oxidative stress and genomic instability (Kennedy et al., 1998; Meyer et al., 2000). In addition, depletion or increased expression of the hMTH1 gene is associated with its crucial roles in avoiding mutagenesis and cell death or senescence (Yoshimura et al., 2003; Nakabeppu et al., 2010). Differential hMTH1 expression is associated with neurodegeneration in humans (Nakabeppu et al., 2010) and carcinogenesis in humans and mice (Kim et al., 2001; Tsuzuki et al., 2001).

In the current study, an AgNP-mediated dose-dependent decrease in hMTH1 gene expression ($\sim$1.8 fold in WT and $\sim$2 fold in KD cells at 0.25 mg/L) in Jurkat T cells was observed (Fig. 4a). Furthermore, alterations in hMTH1 activity, determined as free phosphate release, were evident in both AgNP-exposed WT and KD cells (Fig. 4b). In a similar manner to hOGG1 activity, the release of free phosphate was first increased (at 0.05 mg/L) followed by a decrease with increasing concentrations of AgNP exposures. The diminished expression of hMTH1 at higher concentrations (0.25 mg/L) is most likely linked to AgNP-mediated release of an insufficient amount of free phosphate, which reflects the inefficient activity of hMTH1 at the higher concentration (0.25 mg/L) (Fig. 4b). The suppressed hMTH1 activity was unable to counteract the deleterious AgNP-induced effect of nucleotide pool damage, and ultimately brought about an increase in the 8-OHdG levels in AgNP-treated WT and KD cells. The interaction of silver or other nanoparticles with hMTH1 has not been reported, but it is known that the carcinogenic transition metal ions Ni(II), Cu(II), Co(II), and Cd(II) are able to inhibit both bacterial and human 8-oxo-dGTPases in vitro (Porter et al., 1997; Kasprzak and Bialkowski, 2000). Unlike hOGG1 gene expression, hMTH1 did not display p38 dependency, as there was almost no difference in the magnitude of changes of hMTH1 gene expression or enzyme activity between WT and KD cells in control as well as in AgNP-exposed conditions (Figs. 4a and 4b).

NDX-4, the 8-oxo-dGTPases

Recently, it has been demonstrated that NDX-4 has a MutT-type activity in *C. elegans* that contributes to maintenance of genomic integrity. Moreover, phenotypic analyses suggested that the loss of *ndx-4* leads to an upregulation of key stress response genes that compensate for the in vivo role of *ndx-4* in protection from the deleterious consequences of oxidative stress (Arczewska et al., 2011). In the present study, we found a highly significant ($P < 0.001$) concentration-dependent increase in *ndx-4* gene expression ($\sim$2.4 fold at 0.05 mg/L) (Fig. 4c), and a significant increase ($\sim$2.4 fold at the lower concentration of 0.025 mg/L) followed by a decrease (at 0.05 mg/L) (Fig. 4d) in free phosphate release that actually reflects the 8-oxoGTPases activity of NDX-4 in AgNP-treated WT worms. The changes in *ndx-4* gene expression and enzyme activity in WT worms was similar to that observed for hMTH1, the human counterpart, but the mode of changes were the inverse of each other (i.e., AgNPs suppressed hMTH1 expression in Jurkat T cells, whereas it upregulated *ndx-4* gene expression in *C. elegans*). Since the ortholog of hOGG1 is not yet known in *C. elegans* (Morinaga et al., 2009; Arczewska et al., 2011), it was hypothesized that the worm's 8-oxo-dGTPases (NDX-4) acted as the main defense against AgNP-mediated 8-OHdG accumulation by sanitizing (i.e., removing) oxidized nucleoside triphosphates, such as 8-oxo-dGTPs, from the nucleotide pool.

In contrast to the above, *pmk-1* mutants did not show any changes either in *ndx-4* gene expression or in 8-oxo-dGTPase repair activity after AgNP exposure, except for a slight repression at the highest concentration (0.05 mg/L) of AgNPs (Figs. 4c and 4d), even though no significant differences were observed in the control WT and *pmk-1* mutant worms. The insufficient removal of oxidized nucleotide bases and their eventual incorporation in the newly synthesized DNA due to the diminished 8-oxo-dGTPase repair activity might result in a higher accumulation of 8-OHdG in AgNP-exposed *pmk-1* mutant nematodes (Fig. 2b) compared with WT counterparts. The basal levels of *ndx-4* gene expression and repair activity in WT and *pmk-1* mutant were almost identical to those of their respective controls (Figs. 4c and 4d). Moreover, unlike hMTH1 expression, PMK-1 somehow regulates the expression of NDX-4 following environmental stresses (e.g., AgNPs) but not endogenous oxidative stress. To determine the actual dependency of NDX-4 activity on PMK-1 status, we performed survival tests with *ndx-4* mutants and *ndx-4; pmk-1* RNAi strains. A clear dose-dependent decrease in survival was observed in *ndx-4* mutants following AgNP treatment (Fig. 4e) and, as expected, *ndx-4; pmk-1* RNAi strains showed higher sensitivity than *ndx-4* mutants. The results suggest an interaction between NDX-4 and PMK-1.

It has been suggested that the measurement of a single product (e.g., 8-OHdG) as a biomarker might be misleading because it might not necessarily reflect the overall rate of oxidative DNA damage (Dizdaroglu et al., 2002). The lesion-dependency and substrate specificity of BER pathways, particularly the DNA-glycosylases, may provide further information to elucidate the mechanisms

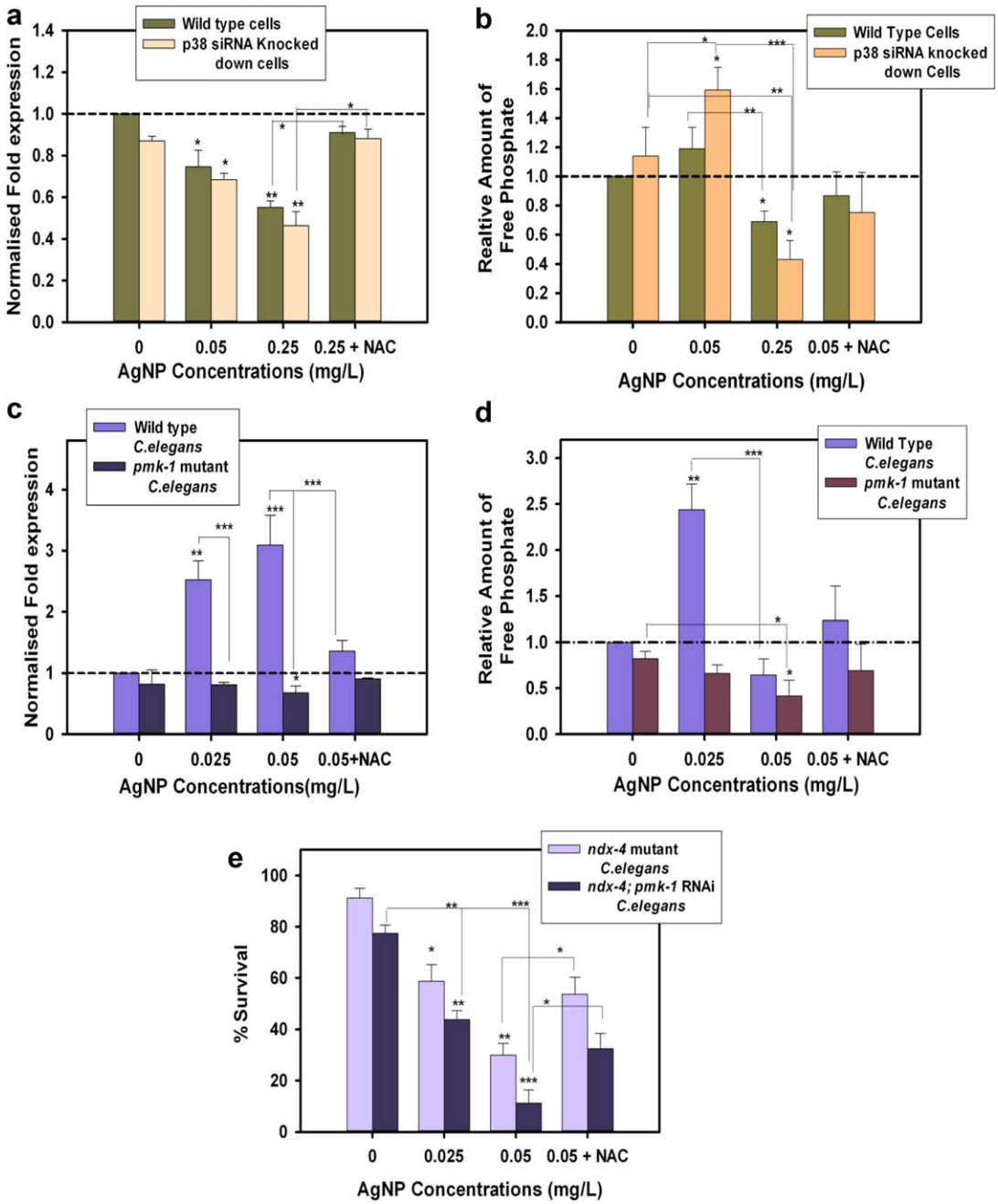

Fig. 4. a. The hMTH1 gene expression in WT and p38 MAPK KD Jurkat T cells following 24 hr AgNP exposure at two different concentrations (0.05 and 0.25 mg/L) measured by qRT-PCR. NAC pretreatment rescued hMTH1 gene expression. Data presented as mean ± SEM. $*P < 0.05$ $**P < 0.001$, $***P < 0.0001$. b. Changes in free phosphate release reflected as hMTH1 repair activity in WT and p38 MAPK KD Jurkat T cells following 24 hr AgNP exposure at two different concentrations (0.05 and 0.25 mg/L). The pyrophosphate, released from the reaction of hMTH1 and the substrate 8-oxo-dGTP, was converted to free phosphate by inorganic pyrophosphatase and the free phosphate was quantified colorimetrically with Biomol Green™. NAC pretreatment rescued the hMTH1 activity. Data presented as mean ± SEM. $*P < 0.05$ $**P < 0.001$, $***P < 0.0001$. c. The *ndx-4* gene expression in WT (*N2*) and *pmk-1* mutant (*km25*) *C. elegans* following 24 hr AgNP exposure at two different concentrations (0.025 and 0.05 mg/L) measured by qRT-PCR. NAC pretreatment rescued *ndx-4* gene expression. Data presented as mean ± SEM. $*P < 0.05$ $**P < 0.001$, $***P < 0.0001$. d. Changes in free phosphate release reflected as NDX-4 repair activity WT (*N2*) and *pmk-1* mutant (*km25*) *C. elegans* following 24 hr AgNP exposure at two different concentrations (0.025 and 0.05 mg/L). The pyrophosphate, released from the reaction of NDX-4 and the substrate 8-oxo-dGTP, was converted to free phosphate by inorganic pyrophosphatase and the free phosphate was quantified colorimetrically with Biomol Green™. NAC pretreatment rescued *ndx-4* repair activity. Data presented as mean ± SEM. $*P < 0.05$ $**P < 0.001$, $***P < 0.0001$. e. Survival (%) of *ndx-4* (*ok1003*) mutants and *ndx-4* (*ok1003*); *pmk-1* RNAi *C. elegans* strains following 24 hr AgNP exposure at two different concentrations (0.025 and 0.05 mg/L) measured by counting the viable and the dead worms by microscopy. NAC pretreatment rescued survival. Data presented as mean ± SEM. $*P < 0.05$ $**P < 0.001$, $***P < 0.0001$. [Color figure can be viewed in the online issue, which is available at wileyonlinelibrary.com.]

involved in DNA damage induction (Rusyn, 2004; Svilar et al., 2011). We thus sought to investigate another DNA-glycosylase, human nth endonuclease III-like 1(*E. coli*) (hNTH1 or hNTHL1) and its ortholog in *C. elegans* (NTH-1), both of which are known for their substrate specificity other than 8-OHdG (e.g., thymine glycol, 5-hydroxycytosine, etc.) (Cooke et al., 2003; Morinaga et al., 2009).

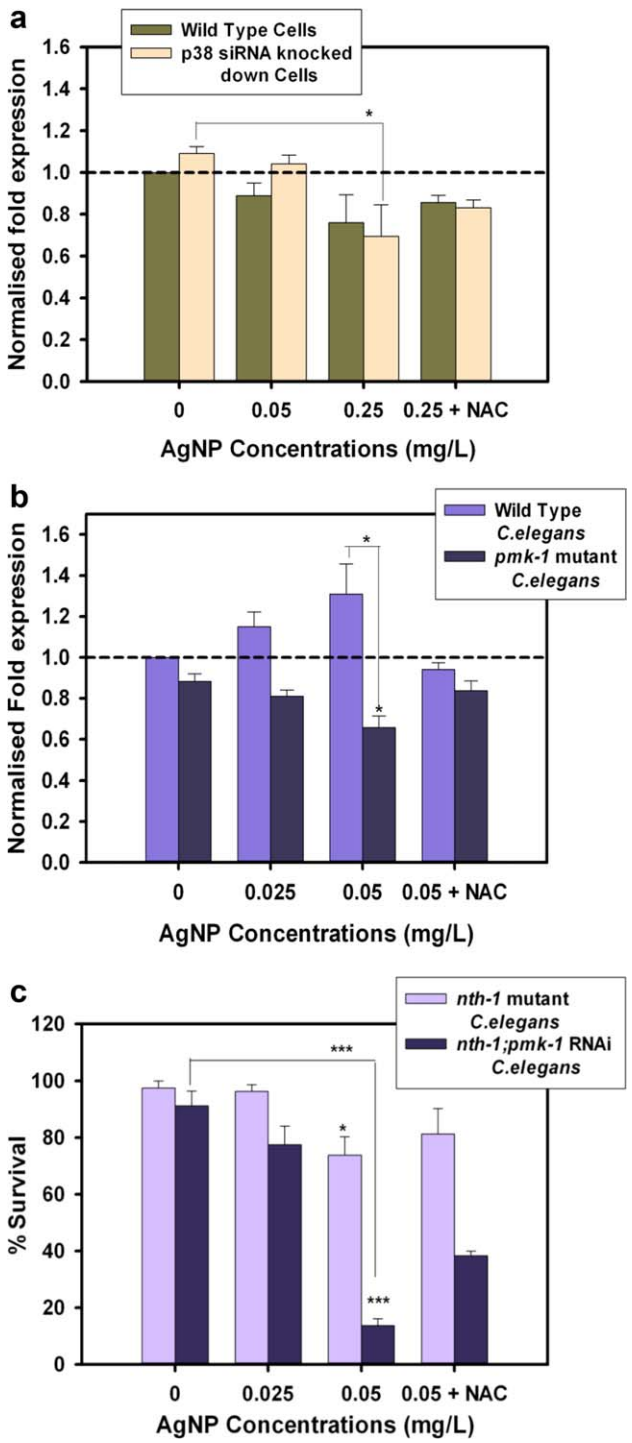

Human nth Endonuclease III-like 1 (*E. coli*) (hNTH1 or hNTHL1)

No remarkable differences in hNTH1 gene expression were found in control or AgNP-treated Jurkat T (WT and KD) cells (Fig. 5A). Only a moderate (~1.3 fold in WT and ~1.4 fold in KD cells) downregulation was observed at the highest concentration (0.25 mg/L) of AgNPs. Furthermore, p38 dependency in hNTH1 expression was not observed as there was almost no difference in hNTH1 gene expression between the control and AgNP-treated WT and p38 MAPK KD Jurkat T cells (Fig. 5A). Hence, hNTH1 does not appear to play a significant role in the removal of AgNP-induced oxidized DNA base lesions.

C.elegans nth Endonuclease III-like 1 (*E.coli*) Homolog (NTH-1)

Consistent with the findings above, *nth-1* gene expression was not affected in *N2* or in *pmk-1* mutant nematodes in controls or AgNP-exposed worms; a small upregulation (~1.35 fold) in *N2* and a moderate downregulation (~1.5 fold) in *pmk-1* mutant strains (Fig. 5B) was observed at the highest (0.05 mg/L) concentration only. A dose-dependent increase in 8-OHdG accumulation and almost no change in *nth-1* gene expressions support the idea that the 8-OHdG might not be a preferred substrate for *nth-1*. Indeed, the order of activity of *nth-1* has been previously reported as Tg/A >> 5-hmU/G > 5-foU/A >> 8-oxoG/G (Morinaga et al., 2009). The relative importance of the *nth-1* gene in BER in *C. elegans* is not yet clear. On one hand, the presence of other DNA-glycosylases has been postulated because no genotoxicant-sensitive phenotypes have been detected in *nth-1* deficient mutants (Meyer et al., 2000; Morinaga et al., 2009; Hunter et al., 2012). On the other hand, Denver et al. (2006) reported that deletion of the *nth-1* gene results in a mutation-prone phenotype. Although we did not find any influence of PMK-1 on *nth-1* gene expression, the levels 8-OHdG were higher (Fig. 2B) in AgNP-treated *pmk-1* mutant worms.

Fig. 5. a. The hNTH1 gene expression in WT and p38 MAPK KD Jurkat T cells following 24 hr AgNP exposure at two different concentrations (0.05 and 0.25 mg/L) measured by qRT-PCR. NAC pretreatment rescued hNTH1 gene expression. Data presented as mean ± SEM. $*P < 0.05$ $**P < 0.001$, $***P < 0.0001$. b. The *nth-1* gene expression in WT (*N2*) and *pmk-1* mutant (*km25*) *C. elegans* following 24 hr AgNP exposure at two different concentrations (0.025 and 0.05 mg/L) measured by qRT-PCR. NAC pretreatment rescued *nth-1* gene expression. Data presented as mean ± SEM. $*P < 0.05$ $**P < 0.001$, $***P < 0.0001$. c. Survival (%) of *nth-1*(*ok724*) mutants and *nth-1*(*ok724*); *pmk-1* RNAi *C. elegans* strains following 24 hr AgNP exposure at two different concentrations (0.025 and 0.05 mg/L) measured by counting the viable and the dead worms by microscopy. Data presented as mean ± SEM. $*P < 0.05$ $**P < 0.001$, $***P < 0.0001$. [Color figure can be viewed in the online issue, which is available at wileyonlinelibrary.com.]

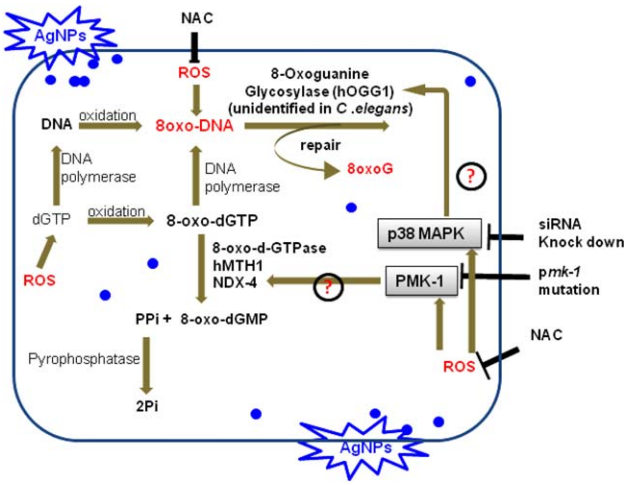

Fig. 6. Possible model of p38 MAPK and PMK-1 mediated AgNPs induced oxidative DNA damage–repair. [Color figure can be viewed in the online issue, which is available at wileyonlinelibrary.com.]

Very slight to almost no change in hNTH1 and NTH-1 reveals that AgNPs did not produce favorable substrates for these repair enzymes (i.e., thymine glycol, 5-hydroxycytosine, etc.) in either of the model systems. To further verify the interaction of *nth-1* and AgNP-exposure and their *pmk-1* dependency, a survival assay with *nth-1* mutant and *nth-1; pmk-1* RNAi strains were carried out. No susceptibility of *nth-1* mutants or *nth-1*; *pmk-1* RNAi strains was found (Fig. 5c), except upon treatment with the highest concentration of AgNPs (0.05 mg/L), which showed a significantly decreased survival of *nth-1*; *pmk-1* RNAi strain (Fig. 5c). We assume that this is due to a PMK-1 RNAi knock-down effect rather than PMK-1 dependency of NTH-1, as it is still comparable with *pmk-1* mutant survival and no difference was found at the lower concentration (0.025 mg/L) as was evident in case of *ndx-4*; *pmk-1* RNAi strains (Fig. 4e).

Clearly, interference with any of the enzymatic steps in the BER pathway could compromise the repair of these oxidative lesions and could potentially promote mutagenesis and, ultimately, cancer development. The exact mechanism of BER inhibition exerted by AgNPs remains to be elucidated. We postulate that the displacement of zinc from DNA glycosylase enzymes might be one important mode of action, as has been reported for metal ions (Asmuss et al., 2000). Unquestionably, throughout all experiments—survival/viability, oxidative DNA damage and repair gene expression, and activity assays—NAC treatment significantly rescued AgNP-mediated toxicity. This observation leads us to conclude that AgNPs cause toxicity through depletion of the antioxidant system, which in turn is protected by p38 MAPK/PMK-1, so that depletion/absence of p38 MAPK/PMK-1 affects viability/survival by affecting the antioxidant reserve. Yamamoto et al. (2007) showed that elevation of glutathione was mediated by p38 MAPK phosphorylation, which in turn caused cytoprotection against oxidative stress in P12 cells (Yamamoto et al., 2007). However, most studies have focused on the depletion of glutathione as the cause of p38 MAPK activation (Limon-Pacheco et al., 2007; Kandil et al., 2010). We present our proposed model for the mechanism of p38 MAPK/PMK-1 in AgNP-induced oxidative DNA damage–repair schematically in Figure 6.

CONCLUSION

In summary, AgNP exposure caused oxidative stress-mediated DNA damage in Jurkat T cell and in the nematode *C. elegans* by affecting DNA glycosylases, specifically hOGG1 and 8-oxo-GTPases, hMTH1, and NDX-4. These findings shed light on the potential for AgNPs to cause carcinogenic effects. Most importantly, p38 MAPK/PMK-1 in combination with oxidative DNA repair proteins counteract AgNP-induced toxicity; modulations of p38 MAPK/PMK-1 caused an increase in the amount of AgNP-induced DNA damage in both mammalian cells and in the nematode. However, given the limitations of the approaches used, it was difficult to pinpoint the exact role of p38 MAPK in oxidative DNA repair systems (i.e., whether the repair enzymes were the direct substrate or were regulated indirectly by p38 MAPK). Nevertheless, our study demonstrates that p38 MAPK and PMK-1 play a protective role in AgNP-induced oxidative DNA damage–repair that is conserved from nematodes to humans.

AUTHOR CONTRIBUTIONS

Prof Dr. Jinhee Choi and Dr. Nivedita Chatterjee designed the study. Dr. Nivedita Chatterjee conducted all the experiments and analyzed the data. Ms. Hyun Jeong Eom contributed with her excellent technical input and expertise. Dr. Nivedita Chatterjee prepared the manuscript draft with important intellectual input from Prof Dr. Jinhee Choi and Ms. Hyun Jeong Eom. All authors approved the final manuscript and had complete access to the study data.

REFERENCES

Ahamed M, Alsalhi MS, Siddiqui MK. 2010a. Silver nanoparticle applications and human health. Clin Chim Acta 411(23-24):1841–1848.

Ahamed M, Karns M, Goodson M, Rowe J, Hussain SM, Schlager JJ, Hong Y. 2008. DNA damage response to different surface chemistry of silver nanoparticles in mammalian cells. Toxicol Appl Pharmacol 233(3):404–410.

Ahamed M, Posgai R, Gorey TJ, Nielsen M, Hussain SM, Rowe JJ. 2010b. Silver nanoparticles induced heat shock protein 70, oxidative stress and apoptosis in Drosophila melanogaster. Toxicol Appl Pharmacol 242(3):263–269.

Arczewska KD, Baumeier C, Kassahun H, Sengupta T, Bjoras M, Kusmierek JT, Nilsen H. 2011. Caenorhabditis elegans NDX-4 is

a MutT-type enzyme that contributes to genomic stability. DNA Repair (Amst) 10(2):176–187.

AshaRani PV, Low Kah Mun G, Hande MP, Valiyaveettil S. 2009. Cytotoxicity and genotoxicity of silver nanoparticles in human cells. ACS Nano 3(2):279–290.

Asmuss M, Mullenders LH, Hartwig A. 2000. Interference by toxic metal compounds with isolated zinc finger DNA repair proteins. Toxicol Lett 112-113:227–231.

Bialkowski K, Kasprzak KS. 1998. A novel assay of 8-oxo-2'-deoxyguanosine 5'-triphosphate pyrophosphohydrolase (8-oxo-dGTPase) activity in cultured cells and its use for evaluation of cadmium(II) inhibition of this activity. Nucleic Acids Res 26(13): 3194–3201.

Brenner S. 1974. The genetics of *Caenorhabditis elegans*. Genetics 77(1):71–94.

Cadet J. 2003. Oxidative damage to DNA: Formation, measurement and biochemical features. Mutat Res/Fund Mol Mech Mutagen 531(1-2):5–23.

Cai W, Rudolph JL, Harrison SM, Jin L, Frantz AL, Harrison DA, Andres DA. 2011. An evolutionarily conserved Rit GTPase-p38 MAPK signaling pathway mediates oxidative stress resistance. Mol Biol Cell 22(17):3231–3241.

Chen X, Schluesener HJ. 2008. Nanosilver: A nanoproduct in medical application. Toxicol Lett 176(1):1–12.

Choi JE, Kim S, Ahn JH, Youn P, Kang JS, Park K, Yi J, Ryu DY. 2010. Induction of oxidative stress and apoptosis by silver nanoparticles in the liver of adult zebrafish. Aquat Toxicol 100(2): 151–159.

Cooke MS, Evans MD, Dizdaroglu M, Lunec J. 2003. Oxidative DNA damage: Mechanisms, mutation, and disease. FASEB J 17(10): 1195–1214.

Coulthard LR, White DE, Jones DL, McDermott MF, Burchill SA. 2009. p38(MAPK): Stress responses from molecular mechanisms to therapeutics. Trends Mol Med 15(8):369–379.

Cuadrado A, Nebreda AR. 2010. Mechanisms and functions of p38 MAPK signalling. Biochem J 429(3):403–417.

Denver DR, Feinberg S, Steding C, Durbin M, Lynch M. 2006. The relative roles of three DNA repair pathways in preventing Caenorhabditis elegans mutation accumulation. Genetics 174(1):57–65.

Dizdaroglu M, Jaruga P, Birincioglu M, Rodriguez H. 2002. Free radical-induced damage to DNA: Mechanisms and measurement. Free Radic Biol Med 32(11):1102–1115.

Ebert F, Weiss A, Bultemeyer M, Hamann I, Hartwig A, Schwerdtle T. 2011. Arsenicals affect base excision repair by several mechanisms. Mutat Res 715(1-2):32–41.

Eom HJ, Ahn JM, Kim Y, Choi J. 2013. Hypoxia inducible factor-1 (HIF-1) - flavin containing monooxygenase-2 (FMO-2) signaling acts in silver nanoparticles and silver ion toxicity in the nematode, Caenorhabditis elegans. Toxicol Appl Pharmacol 270:106–113.

Eom HJ, Choi J. 2010. p38 MAPK activation, DNA damage, cell cycle arrest and apoptosis as mechanisms of toxicity of silver nanoparticles in Jurkat T cells. Environ Sci Technol 44(21): 8337–8342.

Feng QL, Wu J, Chen GQ, Cui FZ, Kim TN, Kim JO. 2000. A mechanistic study of the antibacterial effect of silver ions on Escherichia coli and Staphylococcus aureus. J Biomed Mater Res 52(4):662–668.

Fujikawa K, Kamiya H, Yakushiji H, Fujii Y, Nakabeppu Y, Kasai H. 1999. The oxidized forms of dATP are substrates for the human MutT homologue, the hMTH1 protein. J Biol Chem 274(26): 18201–18205.

Gutierrez-Uzquiza A, Arechederra M, Bragado P, Aguirre-Ghiso JA, Porras A. 2012. p38alpha mediates cell survival in response to oxidative stress via induction of antioxidant genes: Effect on the p70S6K pathway. J Biol Chem 287(4):2632–2642.

Hazra TK, Das A, Das S, Choudhury S, Kow YW, Roy R. 2007. Oxidative DNA damage repair in mammalian cells: A new perspective. DNA Repair (Amst) 6(4):470–480.

Hsin YH, Chen CF, Huang S, Shih TS, Lai PS, Chueh PJ. 2008. The apoptotic effect of nanosilver is mediated by a ROS- and JNK-dependent mechanism involving the mitochondrial pathway in NIH3T3 cells. Toxicol Lett 179(3):130–139.

Hunter SE, Gustafson MA, Margillo KM, Lee SA, Ryde IT, Meyer JN. 2012. In vivo repair of alkylating and oxidative DNA damage in the mitochondrial and nuclear genomes of wild-type and glycosylase-deficient Caenorhabditis elegans. DNA Repair (Amst) 11(11):857–863.

Hwang ET, Lee JH, Chae YJ, Kim YS, Kim BC, Sang BI, Gu MB. 2008. Analysis of the toxic mode of action of silver nanoparticles using stress-specific bioluminescent bacteria. Small 4(6):746–750.

Inoue H, Hisamoto N, An JH, Oliveira RP, Nishida E, Blackwell TK, Matsumoto K. 2005. The C. elegans p38 MAPK pathway regulates nuclear localization of the transcription factor SKN-1 in oxidative stress response. Genes Dev 19(19):2278–2283.

Izumi T, Wiederhold LR, Roy G, Roy R, Jaiswal A, Bhakat KK, Mitra S, Hazra TK. 2003. Mammalian DNA base excision repair proteins: Their interactions and role in repair of oxidative DNA damage. Toxicology 193(1-2):43–65.

Kandil S, Brennan L, McBean GJ. 2010. Glutathione depletion causes a JNK and p38MAPK-mediated increase in expression of cystathionine-gamma-lyase and upregulation of the transsulfuration pathway in C6 glioma cells. Neurochem Int 56(4):611–619.

Kang SJ, Ryoo IG, Lee YJ, Kwak MK. 2012. Role of the Nrf2-heme oxygenase-1 pathway in silver nanoparticle-mediated cytotoxicity. Toxicol Appl Pharmacol 258(1):89–98.

Kannan S, Pang H, Foster DC, Rao Z, Wu M. 2006. Human 8-oxoguanine DNA glycosylase increases resistance to hyperoxic cytotoxicity in lung epithelial cells and involvement with altered MAPK activity. Cell Death Differ 13(2):311–323.

Kasprzak KS, Bialkowski K. 2000. Inhibition of antimutagenic enzymes, 8-oxo-dGTPases, by carcinogenic metals. Recent developments. J Inorg Biochem 79(1-4):231–236.

Kennedy CH, Cueto R, Belinsky SA, Lechner JF, Pryor WA. 1998. Overexpression of hMTH1 mRNA: A molecular marker of oxidative stress in lung cancer cells. FEBS Lett 429(1):17–20.

Kim DH, Feinbaum R, Alloing G, Emerson FE, Garsin DA, Inoue H, Tanaka-Hino M, Hisamoto N, Matsumoto K, Tan MW, et al. 2002. A conserved p38 MAP kinase pathway in Caenorhabditis elegans innate immunity. Science 297(5581):623–626.

Kim HN, Morimoto Y, Tsuda T, Ootsuyama Y, Hirohashi M, Hirano T, Tanaka I, Lim Y, Yun IG, Kasai H. 2001. Changes in DNA 8-hydroxyguanine levels, 8-hydroxyguanine repair activity, and hOGG1 and hMTH1 mRNA expression in human lung alveolar epithelial cells induced by crocidolite asbestos. Carcinogenesis 22(2):265–269.

Kim HR, Kim MJ, Lee SY, Oh SM, Chung KH. 2011. Genotoxic effects of silver nanoparticles stimulated by oxidative stress in human normal bronchial epithelial (BEAS-2B) cells. Mutat Res 726(2):129–135.

Kim JS, Kuk E, Yu KN, Kim JH, Park SJ, Lee HJ, Kim SH, Park YK, Park YH, Hwang CY, et al. 2007. Antimicrobial effects of silver nanoparticles. Nanomedicine 3(1):95–101.

Kondo M, Yanase S, Ishii T, Hartman PS, Matsumoto K, Ishii N. 2005. The p38 signal transduction pathway participates in the oxidative stress-mediated translocation of DAF-16 to Caenorhabditis elegans nuclei. Mech Ageing Dev 126(6-7):642–647.

Lim D, Roh JY, Eom HJ, Choi JY, Hyun J, Choi J. 2012. Oxidative stress-related PMK-1 P38 MAPK activation as a mechanism for toxicity of silver nanoparticles to reproduction in the nematode Caenorhabditis elegans. Environ Toxicol Chem 31(3):585–592.

Limon-Pacheco JH, Hernandez NA, Fanjul-Moles ML, Gonsebatt ME. 2007. Glutathione depletion activates mitogen-activated protein kinase (MAPK) pathways that display organ-specific responses and brain protection in mice. Free Radic Biol Med 43(9):1335–1347.

Liu S-C, Wu H-W, Jiang J-h, Shen G-L, Yu R-Q. 2013. A novel DNAzyme-based colorimetric assay for the detection of hOGG1 activity with lambda exonuclease cleavage. Anal Methods 5(1): 164.

Martindale JL, Holbrook NJ. 2002. Cellular response to oxidative stress: Signaling for suicide and survival. J Cell Physiol 192(1):1–15.

McCubrey JA, Lahair MM, Franklin RA. 2006. Reactive oxygen species-induced activation of the MAP kinase signaling pathways. Antioxid Redox Signal 8(9-10):1775–1789.

Meyer F, Fiala E, Westendorf J. 2000. Induction of 8-oxo-dGTPase activity in human lymphoid cells and normal fibroblasts by oxidative stress. Toxicology 146(2-3):83–92.

Morinaga H, Yonekura S, Nakamura N, Sugiyama H, Yonei S, Zhang-Akiyama QM. 2009. Purification and characterization of Caenorhabditis elegans NTH, a homolog of human endonuclease III: Essential role of N-terminal region. DNA Repair (Amst) 8(7): 844–851.

Nakabeppu Y, Oka S, Sheng Z, Tsuchimoto D, Sakumi K. 2010. Programmed cell death triggered by nucleotide pool damage and its prevention by MutT homolog-1 (MTH1) with oxidized purine nucleoside triphosphatase. Mutat Res 703(1):51–58.

Paz-Elizur T, Sevilya Z, Leitner-Dagan Y, Elinger D, Roisman LC, Livneh Z. 2008. DNA repair of oxidative DNA damage in human carcinogenesis: Potential application for cancer risk assessment and prevention. Cancer Lett 266(1):60–72.

Piao MJ, Kang KA, Lee IK, Kim HS, Kim S, Choi JY, Choi J, Hyun JW. 2011a. Silver nanoparticles induce oxidative cell damage in human liver cells through inhibition of reduced glutathione and induction of mitochondria-involved apoptosis. Toxicol Lett 201(1):92–100.

Piao MJ, Kim KC, Choi JY, Choi J, Hyun JW. 2011b. Silver nanoparticles down-regulate Nrf2-mediated 8-oxoguanine DNA glycosylase 1 through inactivation of extracellular regulated kinase and protein kinase B in human Chang liver cells. Toxicol Lett 207(2):143–148.

Porter DW, Yakushiji H, Nakabeppu Y, Sekiguchi M, Fivash MJ, Jr., Kasprzak KS. 1997. Sensitivity of Escherichia coli (MutT) and human (MTH1) 8-oxo-dGTPases to in vitro inhibition by the carcinogenic metals, nickel(II), copper(II), cobalt(II) and cadmium(II). Carcinogenesis 18(9):1785–1791.

Powell CL, Swenberg JA, Rusyn I. 2005. Expression of base excision DNA repair genes as a biomarker of oxidative DNA damage. Cancer Lett 229(1):1–11.

Rahman MF, Wang J, Patterson TA, Saini UT, Robinson BL, Newport GD, Murdock RC, Schlager JJ, Hussain SM, Ali SF. 2009. Expression of genes related to oxidative stress in the mouse brain after exposure to silver-25 nanoparticles. Toxicol Lett 187(1):15–21.

Roh J-Y, Sim SJ, Yi J, Park K, Chung KH, Ryu D-y, Choi J. 2009. Ecotoxicity of silver nanoparticles on the soil nematode Caenorhabditis elegans using functional ecotoxicogenomics. Environ Sci Technol 43(10):3933–3940.

Rusyn I. 2004. Expression of base excision DNA repair genes is a sensitive biomarker for in vivo detection of chemical-induced chronic oxidative stress: Identification of the molecular source of radicals responsible for DNA damage by peroxisome proliferators. Cancer Res 64(3):1050–1057.

Scown TM, Santos EM, Johnston BD, Gaiser B, Baalousha M, Mitov S, Lead JR, Stone V, Fernandes TF, Jepson M, et al. 2010. Effects of aqueous exposure to silver nanoparticles of different sizes in rainbow trout. Toxicol Sci 115(2):521–534.

Svilar D, Goellner EM, Almeida KH, Sobol RW. 2011. Base excision repair and lesion-dependent subpathways for repair of oxidative DNA damage. Antioxid Redox Signal 14(12):2491–2507.

Troemel ER, Chu SW, Reinke V, Lee SS, Ausubel FM, Kim DH. 2005. p38 MAPK regulates expression of immune response genes and contributes to longevity in C. elegans. PLoS Genetics 2:e183; preprint(2006).

Tsuzuki T, Egashira A, Igarashi H, Iwakuma T, Nakatsuru Y, Tominaga Y, Kawate H, Nakao K, Nakamura K, Ide F, et al. 2001. Spontaneous tumorigenesis in mice defective in the MTH1 gene encoding 8-oxo-dGTPase. Proc Natl Acad Sci U S A 98(20):11456–11461.

Tudek B. 2007. Base excision repair modulation as a risk factor for human cancers. Mol Aspects Med 28(3-4):258–275.

Valavanidis A, Vlachogianni T, Fiotakis C. 2009. 8-hydroxy-2' -deoxyguanosine (8-OHdG): A critical biomarker of oxidative stress and carcinogenesis. J Environ Sci Health C Environ Carcinog Ecotoxicol Rev 27(2):120–139.

Wood RD, Mitchell M, Sgouros J, Lindahl T. 2001. Human DNA repair genes. Science 291(5507):1284–1289.

Yamamoto N, Sawada H, Izumi Y, Kume T, Katsuki H, Shimohama S, Akaike A. 2007. Proteasome inhibition induces glutathione synthesis and protects cells from oxidative stress: Relevance to Parkinson disease. J Biol Chem 282(7):4364–4372.

Yang X, Gondikas AP, Marinakos SM, Auffan M, Liu J, Hsu-Kim H, Meyer JN. 2012. Mechanism of silver nanoparticle toxicity is dependent on dissolved silver and surface coating in Caenorhabditis elegans. Environ Sci Technol 46(2):1119–1127.

Yoshimura D, Sakumi K, Ohno M, Sakai Y, Furuichi M, Iwai S, Nakabeppu Y. 2003. An oxidized purine nucleoside triphosphatase, MTH1, suppresses cell death caused by oxidative stress. J Biol Chem 278(39):37965–37973.

Zarubin T, Han J. 2005. Activation and signaling of the p38 MAP kinase pathway. Cell Res 15(1):11–18.